A Planar Patch Antenna Array for 5G Millimeter Wave Extender

Dushmantha N. Thalakotuna[(1)], Karu P. Esselle [(1)], and Nishat Y. Koli[(1)]
(1) School of Electrical and Data Engineering, Univeristy of Technology Sydney, Sydney, Australia
dushmantha.thalakotuna@uts.edu.au

***Abstract*—A low cost, simple to fabricate, multi-layer printed patch antenna array that can be used as the outdoor antenna system in the 5G Millimeter wave Extender. The antenna is designed to operate in the n258 (24.25 GHz-27.5 GHz) and has a size of 2.3λx2.3λ. The antenna shows 94% efficiency with typical gain of 15.5 dBi with only a 0.6dB gain variation in the band of interest.**

I. INTRODUCTION

Despite the popularity of Millimeter wave (mm-wave), there are certain challenges such as high free space path loss and penetration loss with mm-waves. The free space path loss is about 18 dB higher at 28 GHz compared to 3.5 GHz resulting in a much shorter propagation distance. It is reported that 3.8 cm thick tinted glass result in penetration losses up to 40 dB at 28 GHz [1]. Therefore, additional in-building 5G installations are required to serve indoor users which is expensive and a time consuming task for operators.

A solution to this was first proposed in [2] by the authors. The solution consists of installing a 5G Millimeter wave Extender on the glass or wall of the building so the signals from outdoor gNB. The extender amplifies and relay the signals in the uplink and downlink providing increased signal strength. The 5G extender proposed in [2] has two antenna systems operating at 28 GHz. The outdoor antenna maintain the connectivity to the gNB and the indoor antenna provide coverage for indoor users. In this work, we design a simple low cost printed patch for the outdoor antenna.

II. ANTENNA DESIGN

One of the main considerations for the antenna element is to keep the design simple to fabricate at a low-cost. Thus, patch antenna is considered a suitable candidate. However, a wideband patch design to cover a wideband such as n258 band (24.25 GHz-27.5 GHz) is a challenging task. To overcome this, a stacked patch antenna design undertaken. The structure of a single radiating element is shown in Fig 1.

The radiating patch is sandwiched in between two RO4533 substrate with a dielectric constant of 3.3 and loss tangent 0.0025. A cross slot shown in Fig 1(c) is printed on the upper RO4533 substrate that enhances the matched impedance bandwidth of the radiating patch. The radiating patch design is based on [3] which uses corner cutouts to increase the element bandwidth. The patch is excited using two off centered feed vias for two polarizations as shown in Fig 1(b). The vias are connected to the feed below the ground plane, thus circular cutouts on the ground plane is made to accommodate the feed vias to avoid short circuit connection to the ground. The location of the feed points, patch dimensions are optimized in this design to achieve the required impedance bandwidth. The optimizations were conducted using CST Microwave Studio. The single antenna element has a very wide 10dB impedance bandwidth starting from 24 GHz covering the band of interest from 24.25 GHz-27.5 GHz.

A 4x4 array is implemented using the single antenna element as the base radiating element as shown in Fig 2(a). The element spacing in the array is kept close to λ/2 at the highest frequency of operation. The side lobe reduction is important in the array patterns. A uniform excitation always result in high side lobe levels, therefore an amplitude taper is applied across the antenna array. Considering the feasible track widths for a microstrip feed design, it was decided to excite the edge elements 3dB lower compared to center two elements. The initial array factor evaluation based on single element patterns shows a 5.5 dB reduction in maximum side lobe levels compared to a uniformly excited array

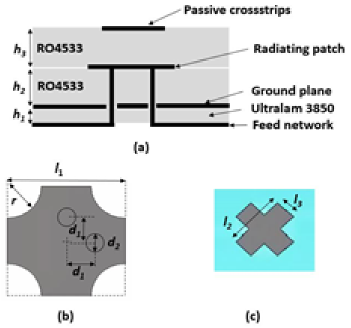

Figure 1. Single antenna element (a) layers (b) radiating patch (c) passive crossstrip. (d_1=0.78mm, h_2=0.6mm, h_1=0.1mm, h_2=0.76mm, h_3=0.76mm, l_1=2.75mm, l_2=3mm, l_3=1mm, r=0.8mm)

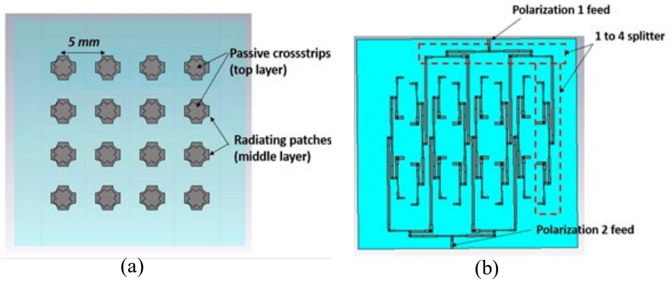

Figure 2. (a) 4x4 antenna array top view. Substrates are transparent to show the radiating patch and passive crossstrips. (b) Feed distribution network.

A 1-16 splitter is designed for each polarization to feed the array elements as shown in Fig. 2(b). This feed network is designed on an Ultralam 3850 laminate with 0.1mm thickness that has a permittivity of 2.9 and loss tangent of 0.0025. The microstrip and the patch antenna array share the same ground plane located beneath the bottom RO4533 substrate.

The antenna array simulated s-parameters are shown in Fig 3. A 10dB impedance match is achieved in the 24.25 GHz- 27.5 GHz band of interest for both polarizations. The cross polarization isolation is worst around 12dB at the start of the band and improves toward the end of the band exceeding 15dB.

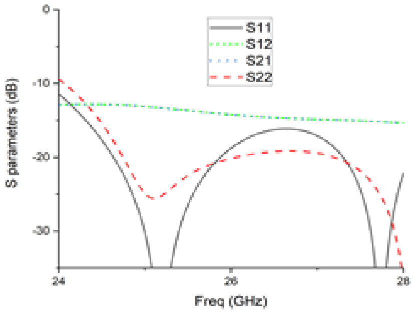

Figure 3. Antenna array simulated scattering parameters

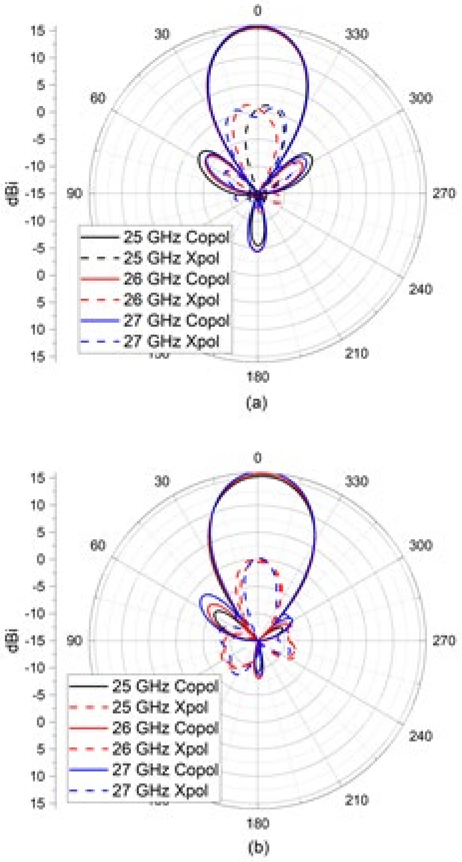

Figure 4. Simulated array patterns (a) Polarization 1 E-plane gain (b) Polarization 2 E-plane gain

The simulated antenna gain patterns for both polarizations are shown in Fig 4 for a few frequency points in the band of interest. The typical gain is about 15.5 dBi for the antenna. The peak gain variation is only about 0.6 dB within the band with a positive slope which is ideal to compensate for the increase in free space attenuation as the frequency increases. The antenna array has a 94% efficiency. The 3dB beamwidth is about 30° in average with ±2° variation at the edges of the band. The worst case side lobe levels in the band of interest are 16dB lower due to the amplitude tapering in the feed network. The 3dB beam squint is within ±0.5° within the band. The worst case cross-polarization is 14dB lower in the broadside direction. The cross-polarization levels at sector edges is not applicable for this applications since this antenna is designed to serve as a direct point to point link rather than serving users.

III. CONCLUSION

The 5G extender overcomes the millimeter wave propagation challenges by acting as an intermediary amplifier to segue the signal in uplink and downlink. This require a high gain, wideband, low cost and simple to fabricate antenna for outdoor antenna system. In this work we have designed and evaluated the performance of a patch antenna array that meets these requirements. The array is based on a multilayer patch antenna element with a passive reflector crossstrips. The circular cutouts in the patch combined with the reflector crossstrips help to achieve a wide impedance bandwidth from 24.25 GHz-27.5 GHz compared to narrow bandwidths achieved from conventional patch antenna elements.

The average cross polarization isolation level in the array is 15dB but due to the size, separate arrays for each polarization can be used if higher isolation is required. The current design shows typical gain of 15.5 dBi and higher gains can be achieved by designing a larger array if needed. However this can lead to challenges during the 5G extender setup. In particular, the smaller beamwidth can lead to difficulties in pointing/aligning the antenna to gNB during the installation. The 3dB beam squint is within 0.5° in the entire band removing the need to realign the antenna depending on the frequency of use. The crosspolarization levels and side lobe levels remain 14dB and 16dB lower respectively in the worst case.

ACKNOWLEDGMENT

The authors would like to acknowledge the financial support provided by the Australian Government under the Australian Research Council Discovery Grant scheme and a University of Technology Sydney Faculty of Engineering & IT seed grant.

REFERENCES

[1] T. S. Rappaport, R. W. Heath, R. C. Daniels and J. N. Murdock, Millimeter Wave Wireless Communications, 1st ed., Upper Saddle River, NJ: Prentice Hall, 2014.

[2] Dushmantha N.P. Thalakotuna, Karu P. Esselle, "Overcoming 5G Millimeter Wave Black Holes", IEEE Future Networks Tech Focus, Volume 3, Issue 3, November 2019.

[3] K. Klionovski and A. Shamim, "Physically Connected Stacked Patch Antenna Design With 100% Bandwidth," in IEEE Antennas and Wireless Propagation Letters, vol. 16, pp. 3208-3211, 2017.